

Published in final edited form as:

*J Orthop Res.* 2010 July ; 28(7): 928–936. doi:10.1002/jor.21078.

## Modulation of Wnt Signaling Influences Fracture Repair

David E. Komatsu<sup>1</sup>, Michelle N. Mary<sup>1</sup>, Robert Jason Schroeder<sup>1</sup>, Alex G. Robling<sup>2</sup>, Charles H. Turner<sup>3</sup>, and Stuart J. Warden<sup>2,3,4</sup>

<sup>1</sup>InMotion Orthopaedic Research Center, 20 South Dudley, Suite 700, Memphis, Tennessee 38103

<sup>2</sup>Department of Anatomy and Cell Biology, Indiana University School of Medicine, 635 Barnhill Drive, MS-5035, Indianapolis, Indiana 46202

<sup>3</sup>Department of Biomedical Engineering, Purdue School of Engineering and Technology, Indiana University—Purdue University Indianapolis, 1120 South Drive, FH-115, Indianapolis, Indiana 46202

<sup>4</sup>Department of Physical Therapy, School of Health and Rehabilitation Sciences, Indiana University, 1140 W. Michigan Street, CF-326, Indianapolis, Indiana 46202

### Abstract

While the importance of Wnt signaling in skeletal development and homeostasis is well documented, little is known regarding its function in fracture repair. We hypothesized that activation and inactivation of Wnt signaling would enhance and impair fracture repair, respectively. Femoral fractures were generated in *Lrp5* knockout mice (*Lrp5*<sup>-/-</sup>) and wild-type littermates (*Lrp5*<sup>+/+</sup>), as well as C57BL/6 mice. *Lrp5*<sup>-/-</sup> and *Lrp5*<sup>+/+</sup> mice were untreated, while C57BL/6 mice were treated 2×/week with vehicle or anti-Dkk1 antibodies (Dkk1 Ab) initiated immediately postoperatively (Day 0) or 4 days postoperatively (Day 4). Fractures were radiographed weekly until sacrifice at day 28, followed by DXA, pQCT, and biomechanical analyses. *Lrp5*<sup>-/-</sup> mice showed impaired repair compared to *Lrp5*<sup>+/+</sup> mice, as evidenced by reduced callus area, BMC, BMD, and biomechanical properties. The effects of Dkk1 Ab treatment depended on the timing of initiation. Day 0 initiation enhanced repair, with significant gains seen for callus area, BMC, BMD, and biomechanical properties, whereas Day 4 initiation had no effect. These results validated our hypothesis that Wnt signaling influences fracture repair, with prompt activation enhancing repair and inactivation impairing it. Furthermore, these data suggest that activation of Wnt signaling during fracture repair may have clinical utility in facilitating fracture repair.

### Keywords

Wnt; fracture repair; Dkk1; *Lrp5*

The canonical Wnt signaling pathway has rapidly emerged as a vital regulator of skeletal development, homeostasis, and mechanotransduction.<sup>1,2</sup> Activation of this pathway begins with the binding of Wnt ligands to the extracellular domains of the Wnt coreceptors, low-density lipoprotein receptor-related protein 5/6 (LRP5/6) and Frizzleds (Fz1-10). Following receptor binding, inhibition of glycogen-synthase kinase 3 (Gsk3) results in the accumulation and nuclear translocation of hypophosphorylated  $\beta$ -catenin where it binds to

members of the TCF/LEF family of transcription factors to direct the transcription of Wnt responsive genes.<sup>2</sup>

Clinical interest in this pathway was sparked by the discovery that osteoporosis pseudoglioma (OPPG), a disease characterized by low bone mass and recurrent fractures, was caused by loss of function mutations in LRP5.<sup>3</sup> Shortly after this discovery, a gain-of-function mutation in LRP5 was identified that confers a high bone mass phenotype.<sup>4,5</sup> Transgenic mouse models incorporating these mutations recapitulate the human skeletal phenotypes. Lrp5 knockout mice (Lrp5<sup>-/-</sup>) display decreases in bone mass, mechanical properties, and mechanosensitivity.<sup>6-8</sup> Conversely, mice engineered with Lrp5 gain-of-function mutations display increases in bone mass and biomechanical properties, along with possible increases in mechanosensitivity.<sup>9-12</sup> The clinical and animal data highlight the clinical potential of Wnt modulation for treating skeletal disease and injury, and the complex regulation of this pathway presents a wide variety of specific therapeutic targets.

The predominant Wnt regulators comprise several families of secreted proteins including Dickkopf 1 and 2 (Dkk1 and Dkk2), sclerostin, Wnt-1-induced secreted protein (WISE), Wnt inhibitory factor 1 (Wif-1), and secreted frizzled related proteins (sFRPs).<sup>2</sup> Wif-1 and sFRPs regulate Wnt signaling by competitively binding Wnt ligands, whereas Dkk1 and sclerostin bind to LRP5/6, thereby inhibiting Wnt signal transduction.<sup>2</sup> Treatment of rats and mice with neutralizing antibodies to Dkk1 (Dkk1 Ab) is anabolic at both cortical and trabecular sites.<sup>13</sup> In addition, Wnt activation by Gsk3 inhibitors and LiCl is anabolic in Lrp5<sup>-/-</sup> mice, osteopenic SAMP6 mice, and ovariectomized rats.<sup>7,14</sup> Although osteoporosis represents the largest market for skeletal anabolics, the potential of Wnt activation to benefit fracture patients represents a significant secondary market.

The first report of Wnt involvement in fracture repair came from a rat fracture study that identified transcriptional upregulation of Wnt-5a, Fz and  $\beta$ -catenin, as well as several target genes during this process.<sup>15</sup> A follow-up study revealed upregulation of Lrp5 in fracture callus mRNA and localized  $\beta$ -catenin expression in the callus to proliferating chondrocytes, osteoblasts, and periosteal osteoprogenitor cells, indicating that Wnt signaling is active in endochondral and intramembranous ossification.<sup>16</sup> Subsequent researchers showed that targeted disruption of  $\beta$ -catenin or overexpression of Dkk1 virtually abrogated the reparative process, whereas Wnt activation by LiCl treatment enhanced fracture repair.<sup>17</sup> Surprisingly, the early phase of fracture repair in mice with Lrp5 gain-of-function mutations is impaired, attributed to an increase in cell proliferation and concomitant delay in osteoblast differentiation.<sup>18</sup>

To further understanding of Wnt signaling in fracture repair, we performed a series of closed femoral fracture experiments in Lrp5<sup>-/-</sup> mice and wild-type littermates, as well as C57BL/6 mice treated with Dkk1 Ab. Using biomechanical integrity as the primary outcome measure, we hypothesized that inhibition of Wnt signaling by Lrp5 deletion would impair fracture repair. Conversely, we hypothesized that neutralization of Dkk1-mediated Wnt inhibition by systemic treatment with Dkk1 Ab would enhance fracture repair.

## METHODS

### Animal Model

Male and female Lrp5-deficient mice (Lrp5<sup>-/-</sup>) and wild-type littermates (Lrp5<sup>+/+</sup>) were obtained by breeding heterozygous Lrp5 mice, as previously described,<sup>12</sup> and male C57BL/6 mice were purchased from Jackson Labs (Bar Harbor, ME). At 17 weeks of age, they were subjected to unilateral closed femoral fractures using previously described methods.<sup>19</sup> This fracture model involves soft tissue injury, rigid fixation, and the development of a large

fracture callus, all of which are consistent with the indirect mode of healing seen in well-fixed traumatic fractures that are of interest in this study. Although this model is associated with higher variability than open osteotomy or defect models of bone healing, because these models require opening of the muscle envelope and periosteal disruption, they are better suited for studying the direct mode of bone healing seen subsequent to surgical procedures. Analgesia (Buprenex, 0.05 mg/kg; Reckitt Benckiser, Richmond, VA) was provided intraoperatively and at 12, 24, and 36 h postoperatively. The Lrp5<sup>-/-</sup> and Lrp5<sup>+/+</sup> mice (male Lrp5<sup>-/-</sup>,  $N=13$ , weight =  $24.17 \pm 1.22$  g; male Lrp5<sup>+/+</sup>,  $N=16$ , weight =  $25.45 \pm 2.10$  g; female Lrp5<sup>-/-</sup>,  $N=12$ , weight =  $21.30 \pm 1.86$  g; female Lrp5<sup>+/+</sup>,  $N=9$ , weight =  $21.06 \pm 1.72$  g) received no treatment while the C57BL/6 mice (weight =  $29.04 \pm 1.40$  g) were subjected to one of three treatments: 1) Vehicle (PBS, 2 $\times$ /week, initiated immediately postop,  $N=9$ ); 2) Dkk1 Ab Day 0 (25 mg/kg s.c., 2 $\times$ /week, initiated immediately postop,  $N=9$ ); 3) Dkk1 Ab Day 4 (25 mg/kg s.c., 2 $\times$ /week, initiated 4 days postop,  $N=8$ ). At 4 weeks postop, all animals were euthanized, and the fractured and contralateral intact (control) femurs were harvested and the pins removed. All procedures were approved by the Indiana University IACUC prior to study commencement.

### Longitudinal Radiography

High-resolution digital X-rays (piXarray100, Micro Photonics Inc., Allentown, PA) were acquired immediately following fracture and weekly thereafter. Images from weeks 2, 3, and 4 were analyzed using Image J (Version 1.40g, NIH, Bethesda, MD) to quantify projected callus area by fitting a spline to the outer callus boundary and recording the area in pixels. These values were then converted to mm<sup>2</sup> by referencing a calibration phantom.

### Densitometry

The bone mineral density (BMD), bone mineral content (BMC), and area of isolated fractured and intact femurs was determined by dual-energy X-ray absorptiometry (DXA) using a PIXImus II (GE-Lunar, Madison, WI). Peripheral quantitative computed tomography (pQCT) analyses were then conducted using a Stratec XCT Research SA+ pQCT (Stratec, Pforzheim, Germany). Three slices, positioned at the center of the fracture, and 0.5 mm proximal and distal, were acquired for each fractured femur. For the contralateral intact femurs, three slices were acquired at the same relative position. Scans of fractured femurs were analyzed for total callus area and density at a threshold of 250 mg/cm<sup>3</sup>, and mature callus area and density at a threshold of 600 mg/cm<sup>3</sup>. Intact femurs were analyzed for total area and density at a threshold of 600 mg/cm<sup>3</sup>.

### Biomechanical Testing

Following rehydration and equilibration to room temperature, femurs were positioned, anterior surface up, in a 4-point loading jig (10 mm outer span, 4 mm inner span) with the fractures centered between the inner points. A monotonic load to failure was applied to the anterior surface at 0.1 mm/min, under displacement control, using an EnduraTEC ELF3200 equipped with a 225 N load cell (Bose, Eden Prairie, MN) and running WinTest (Ver. 2.54, Bose). Force and displacement data were exported to Excel (Microsoft, Redmond, WA) and used to plot loading curves. Energy to failure (mJ), stiffness (N/mm), and ultimate force (N) were then calculated using a set of custom written macros. In order to determine stiffness, the slope of the loading curves was calculated in linear regions between the initial toe and the yield point. The selection of points was made by a blinded experimenter and encompassed the largest portion of the loading curve possible for each sample.

## Statistical Analysis

Results of DXA, pQCT, and biomechanics analyses of fractured Lrp5<sup>-/-</sup> and Lrp5<sup>+/+</sup> femurs were normalized to their contralateral intact femurs to account for baseline genotypic differences. Effects of sex and genotype were assessed using two-way ANOVA models. Since none of the interaction terms were significant, only main effects were included. Responses of intact and fractured femurs from vehicle and Dkk1 Ab-treated mice were compared separately using one-way ANOVA models, with pair-wise comparisons between vehicle and each treatment group made using Dunnett's procedure. All analyses were carried out using *R*, and *p*-values less than 0.05 were considered significant.

## RESULTS

At week 1, no significant callus development was apparent in any of the groups (Fig. 1), so this time-point was not analyzed. From weeks 2 to 4, a near linear decrease in callus size was seen for all groups (Fig. 2). At all three time-points, calluses from male and female Lrp5<sup>-/-</sup> mice were significantly smaller (~25%) than wild-type controls. In addition, calluses from female mice were ~20% smaller than those from males, though this was only significant at week 3 (*p*=0.0273). The Dkk1 Ab Day 0 group displayed a dramatic effect, with significant increases in callus size, averaging 52% across all time points, compared to vehicle controls. In contrast, Dkk1 Ab Day 4 mice showed no differences from controls.

Postnecropsy DXA analyses of intact femora confirmed prior reports of decreased BMD and BMC in Lrp5<sup>-/-</sup> mice<sup>7,8</sup> (Table 1). In order to isolate the effects of Lrp5 deletion on fracture repair from the underlying phenotype, all further results for fractured femora from Lrp5<sup>-/-</sup> and Lrp5<sup>+/+</sup> mice were normalized to their contralateral intact femora (see Table 1 for the actual values for all parameters). DXA analysis of fractured femurs from Lrp5<sup>-/-</sup> mice revealed significant reductions in BMD (10%), BMC (15%), and area (2%), as compared to Lrp5<sup>+/+</sup> mice, with no effects observed for sex (Fig. 3A–C). Dkk1 Ab treatment affected DXA-determined properties of both intact and fractured femora, and these results were dependent on the timing of treatment initiation. In Dkk1 Ab Day 0 mice, intact femoral BMD and BMC significantly increased by 6% and 11%, respectively, as compared to vehicle controls (Fig. 3D–F). Likewise, the BMD and BMC of fractured femora increased 15% and 23%, respectively. In contrast, intact femora from Dkk1 Ab Day 4 mice suffered from an ~10% reduction in BMD and BMC, whereas their fractured femora were indistinguishable from vehicle controls.

As planar radiography and DXA generate generalized, two-dimensional information, pQCT was used to determine cross-sectional properties of intact femora and fracture calluses. Similar to the DXA analysis, intact femora from Lrp5 mice were smaller and less mineralized (Table 1). No significant genotype or sex effects were seen for density, but significant reductions of ~20% in both total and mature callus area were observed for Lrp5 deficiency and female sex (Fig. 4A–D). Treatment with Dkk1 Ab also significantly affected callus area, with calluses from Dkk1 Ab Day 0 mice characterized by 58% more total and 29% more mature callus area, though no differences were seen for density (Fig. 4E, F). Consistent with radiographic and DXA observations, Dkk1 Ab Day 4 mice had no changes in fracture callus area or density, but again displayed catabolic responses in intact femora with reductions in cross-sectional area and density of 14% and 6%, respectively.

The most important outcome in fracture repair is restoration of biomechanical integrity. Therefore, 4-point bending tests were conducted on the isolated femurs. As expected, the biomechanical properties of intact femora from Lrp5<sup>-/-</sup> mice were compromised (Table 1). In addition, Lrp5 deficiency significantly diminished the mechanical properties of fractured femurs as evidenced by losses of 48%, 38%, and 26% in energy to failure, ultimate force,

and stiffness, respectively (Fig. 5A–C). A sex effect was also observed with female mice showing a 35% reduction in energy to failure. Intact femurs from Dkk1Ab Day 0 mice showed significant biomechanical gains for ultimate force (9%) and stiffness (25%), whereas those from Dkk1 Day 4 mice were marked by a significant 13% reduction in ultimate force (Fig. 5D–F). Likewise, the effects on fractured femurs were affected by the timing of dose initiation, with Dkk1 Ab Day 0 mice demonstrating a 27% increase in ultimate force and a 40% increase in stiffness, whereas those from Dkk1 Ab Day 4 mice were biomechanically indistinguishable from vehicle controls.

## DISCUSSION

These experiments sought to test the complementary hypotheses that Lrp5 deletion adversely affects fracture repair and Dkk1 Ab treatment enhances this process. Overall, the results obtained support these hypotheses, as fractured femurs from Lrp5<sup>-/-</sup> mice were smaller, less mineralized, and biomechanically inferior to those from wild-type littermates. Conversely, treatment with Dkk1 Ab increased the size, mineralization, and biomechanical properties of fractured femurs, though this was only seen when treatment was initiated immediately postoperatively.

These data represent the first direct evidence that deletion of Lrp5 delays the restoration of biomechanical integrity during fracture repair. However, others have documented the importance of other Wnt pathway members in this process. Chen et al.<sup>17</sup> performed a series of murine tibial fracture experiments in which targeted  $\beta$ -catenin disruption and Dkk1 overexpression were used to repress Wnt signaling and observed gross impairment of the reparative process. Similarly, overexpression of Dkk1 has also been shown to impair bone regeneration in murine tibial defects.<sup>18</sup> Dkk1 inhibits Wnt signaling by binding to both Lrp5 and Lrp6 to prevent formation of the Frizzled/Lrp5/6 complex, as well as by binding to Kremen, leading to the internalization of Lrp5/6.<sup>1</sup> As such, studies utilizing Dkk1 overexpression to inactivate Wnt signaling cannot discriminate between the relative contributions of Lrp5 and Lrp6 to Wnt signal transduction in fracture repair and, similar to  $\beta$ -catenin disruption, solely implicate canonical Wnt signaling as vital to successful fracture repair. By utilizing Lrp5<sup>-/-</sup> mice, the results of these experiments reveal that Lrp5 is required for the timely restoration of biomechanical integrity during fracture repair. However, as the biomechanical analyses were conducted solely on day 28, further studies will be required to ascertain if fracture repair in these mice is delayed or impaired. In addition, the necessity of Lrp6 in fracture repair, as well as the degree to which the loss of one of these receptors can be compensated for by the other, remains to be elucidated.

The recent finding that the low bone mass phenotype of Lrp5<sup>-/-</sup> mice is caused by excessive serotonin synthesis in the duodenum,<sup>20</sup> and strong clinical evidence that selective serotonin reuptake inhibitor use is associated with skeletal fragility and increased fracture risk,<sup>21</sup> indicates that impaired fracture repair in Lrp5<sup>-/-</sup> mice may not solely be due to Wnt inactivation at the fracture site. However, as osteoblast-specific  $\beta$ -catenin knockdown and local Dkk1 delivery both impair fracture repair,<sup>17,18</sup> it is reasonable to posit that Wnt inactivation in callus osteoblasts and/or chondrocytes does contribute to the disruption in fracture repair seen in Lrp5<sup>-/-</sup> mice. Moreover, bone marrow cells harvested from Lrp5<sup>-/-</sup> mice produce fewer alkaline phosphatase-positive colonies,<sup>6</sup> indicating that Lrp5 deletion affects the proliferation of osteoblast precursors independent of serotonin levels. Nevertheless, because this study was not designed to determine the relative contributions of gut and fracture callus Lrp5 insufficiency, further studies will be required to resolve this issue definitively.

Interestingly, the utilization of radiographic (i.e., X-rays, DXA, and pQCT) and biomechanical outcome measures revealed a discrepancy in the magnitude of impairment seen in *Lrp5*<sup>-/-</sup> mice. While radiographic measures of repair showed average losses of 15%, biomechanical losses averaged 40%. This suggests that *Lrp5*-mediated Wnt signaling is less important to simple mineral accrual at the fracture site than it is to restoring proper structural arrangement of this material. Several aspects of Wnt signaling likely underlie this finding. First, Wnt signaling is critical to embryonic limb patterning, with precise spatiotemporal activation required for proper organization of nascent skeletal structures.<sup>22</sup> Accordingly, improper collagen organization could result in adequately mineralized but structurally weak calluses. Second, Wnt signaling upregulates *Dkk2*, a protein not required for osteoid production but necessary for subsequent mineralization.<sup>2</sup> Reduced *Dkk2* expression in *Lrp5*<sup>-/-</sup> calluses could therefore have resulted in large amounts of unmineralized osteoid that was radiographically indistinguishable from fully mineralized callus. Finally, because Wnt signaling also upregulates osteoprotegerin (OPG),<sup>2</sup> decreased OPG expression in *Lrp5*<sup>-/-</sup> calluses may have resulted in early initiation of osteoclastogenesis. Therefore, premature fracture site resorption may also have contributed to the discrepancy between biomechanical and radiographic losses seen in *Lrp5*<sup>-/-</sup> mice.

Comparisons between male and female mice indicate that *Lrp5* deficiency is more detrimental to fracture repair in females. These findings are consistent with prior work demonstrating that females are more susceptible to alterations in Wnt signaling as evidenced by greater suppression of load-induced bone formation in female *Lrp5*<sup>-/-</sup> mice<sup>8</sup> and a more severe bone phenotype in female mice haploinsufficient for *Lef1* and *Gsk3 $\beta$* .<sup>23</sup> These sex effects may be due to cross-talk between estrogen and Wnt signaling<sup>24</sup> and, given the potentially significant clinical ramifications of any such interactions, further research into this area is clearly warranted.

While the identification of *Lrp5* as a key constituent of fracture repair provides circumstantial evidence that Wnt targeted therapeutics may have clinical utility in enhancing fracture repair, the significant gains seen for virtually all outcomes in the *Dkk1* Ab Day 0 mice provide direct evidence of this. This is not the first study to link Wnt activation with enhanced fracture repair, as LiCl, a *Gsk3* inhibitor, has also been shown to enhance fracture repair.<sup>17</sup> However, *Dkk1* Ab solely target the Wnt pathway, whereas LiCl also exerts skeletal activity through induction of parathyroid hormone<sup>7</sup> and inhibition of 1,25(OH)<sub>2</sub>D<sub>3</sub>-induced resorption,<sup>25</sup> so the effects of LiCl treatment on fracture repair may not result solely from Wnt activation. These Wnt-independent effects of LiCl treatment may explain the differences in outcomes between our results and those seen for LiCl.<sup>17</sup> The major differences between these studies are the differential responses due to timing of treatment initiation. LiCl enhanced fracture repair when initiated 4 days postoperatively, yet impaired the process when treatment began 2 weeks prior to fracture induction.<sup>17</sup> In contrast, *Dkk1* treatment was beneficial when initiated immediately postoperatively, but had no efficacy when initiated 4 days postoperatively. The authors of the LiCl study suggest that Wnt activation inhibits osteoblast differentiation, thereby impairing fracture repair following preoperative initiation due to lack of osteoblast differentiation. This reasoning is supported by evidence that mesenchymal precursors exposed to Wnt3a, or engineered with constitutively active *Lrp5* mutations, do not differentiate into osteoblasts and instead remain in a proliferative state.<sup>2,18</sup> However, others have reported that mesenchymal cells treated with LiCl or engineered to overexpress Wnt3a or stabilized  $\beta$ -catenin undergo more rapid differentiation into mature osteoblasts.<sup>3,7</sup> As inhibition and induction of mesenchymal differentiation by Wnt signaling supports the LiCl results and our *Dkk1* results, respectively, these divergent data underscore the complexity of Wnt signaling in fracture repair.

The catabolic effects seen in the intact femora from Dkk1 Ab Day 4 mice were completely unexpected. Prior studies have shown that Dkk1 Ab are anabolic at both cortical and trabecular sites,<sup>13</sup> and able to inhibit multiple myeloma-induced bone resorption and tumor growth,<sup>26</sup> indicating that Dkk1 inhibition can both inhibit bone resorption and promote bone formation. In light of these data, the cause underlying the presumed systemic increase in bone resorption that was observed in these animals is unclear. However, it is clear that proper timing is tantamount for Wnt targeted therapeutics to be of clinical utility in enhancing fracture repair.

In summary, this study has conclusively demonstrated that Lrp5 is required for successful fracture repair, and that properly timed activation of Wnt signaling has promising clinical utility for enhancing this process. Further studies designed to elucidate the molecular mechanisms underlying the outcomes reported in this study, as well as determine the precise levels of Wnt signaling activity in the calluses of Lrp5<sup>-/-</sup> and Dkk1 Ab-treated mice, will better clarify the potential of targeting this pivotal pathway and harnessing it for clinical benefit in the treatment of fractures.

## Acknowledgments

The Dkk1 antibodies used in this study were kindly supplied by Amgen, Inc. Funding for this study was provided by a National Institutes of Health research grant (R01-AR53237).

## References

1. Johnson ML, Harnish K, Nusse R, et al. LRP5 and Wnt signaling: a union made for bone. *J Bone Miner Res.* 2004; 19:1749–1757. [PubMed: 15476573]
2. Macsai CE, Foster BK, Xian CJ. Roles of Wnt signaling in bone growth, remodeling, skeletal disorders and fracture repair. *J Cell Physiol.* 2008; 215:578–587. [PubMed: 18247365]
3. Gong Y, Slee RB, Fukai N, et al. LDL receptor-related protein 5 (LRP5) affects bone accrual and eye development. *Cell.* 2001; 107:513–523. [PubMed: 11719191]
4. Little RD, Carulli JP, Del Mastro RG, et al. A mutation in the LDL receptor-related protein 5 gene results in the autosomal dominant high-bone-mass trait. *Am J Hum Genet.* 2002; 70:11–19. [PubMed: 11741193]
5. Boyden LM, Mao J, Belsky J, et al. High bone density due to a mutation in LDL-receptor-related protein 5. *N Engl J Med.* 2002; 346:1513–1521. [PubMed: 12015390]
6. Kato M, Patel MS, Lévassieur R, et al. Cbfa1-independent decrease in osteoblast proliferation, osteopenia, and persistent embryonic eye vascularization in mice deficient in Lrp5, a Wnt coreceptor. *J Cell Biol.* 2002; 157:303–314. [PubMed: 11956231]
7. Clément-Lacroix P, Ai M, Morvan F, et al. Lrp5-independent activation of Wnt signaling by lithium chloride increases bone formation and bone mass in mice. *Proc Natl Acad Sci USA.* 2005; 102:17406–17411. [PubMed: 16293698]
8. Sawakami K, Robling AG, Ai M, et al. The Wnt co-receptor LRP5 is essential for skeletal mechanotransduction but not for the anabolic bone response to parathyroid hormone treatment. *J Biol Chem.* 2006; 281:23698–23711. [PubMed: 16790443]
9. Johnson ML, Picconi JL, Recker RR. The gene for high bone mass. *Endocrinologist.* 2002; 12:445–453.
10. Babij P, Zhao W, Small C, et al. High bone mass in mice expressing a mutant LRP5 gene. *J Bone Miner Res.* 2003; 18:960–974. [PubMed: 12817748]
11. Akhter MP, Wells DJ, Short SJ, et al. Bone biomechanical properties in LRP5 mutant mice. *Bone.* 2004; 35:162–169. [PubMed: 15207752]
12. Robinson JA, Chatterjee-Kishore M, Yaworsky PJ, et al. Wnt/beta-catenin signaling is a normal physiological response to mechanical loading in bone. *J Biol Chem.* 2006; 281:31720–31728. [PubMed: 16908522]

13. Grisanti M, Niu QT, Fan W, et al. Dkk-1 inhibition increases bone mineral density in rodents. *J Bone Miner Res.* 2006; 21:S25.
14. Kulkarni NH, Onyia JE, Zeng Q, et al. Orally bioavailable GSK-3alpha/beta dual inhibitor increases markers of cellular differentiation in vitro and bone mass in vivo. *J Bone Miner Res.* 2006; 21:910–920. [PubMed: 16753022]
15. Hadjiargyrou M, Lombardo F, Zhao S, et al. Transcriptional profiling of bone regeneration. Insight into the molecular complexity of wound repair. *J Biol Chem.* 2002; 277:30177–30182. [PubMed: 12055193]
16. Zhong N, Gersch RP, Hadjiargyrou M. Wnt signaling activation during bone regeneration and the role of dishevelled in chondrocyte proliferation and differentiation. *Bone.* 2006; 39:5–16. [PubMed: 16459154]
17. Chen Y, Whetstone HC, Lin AC, et al. Beta-catenin signaling plays a disparate role in different phases of fracture repair: implications for therapy to improve bone healing. *PLoS Med.* 2007; 4:1216–1229.
18. Kim JB, Leucht P, Lam K, et al. Bone regeneration is regulated by Wnt signaling. *J Bone Miner Res.* 2007; 22:1913–1923. [PubMed: 17696762]
19. Komatsu DE, Bosch-Marce M, Semenza GL, et al. Enhanced bone regeneration associated with decreased apoptosis in mice with partial HIF-1alpha deficiency. *J Bone Miner Res.* 2007; 22:366–374. [PubMed: 17181398]
20. Yadav VK, Ryu JH, Suda N, et al. Lrp5 controls bone formation by inhibiting serotonin synthesis in the duodenum. *Cell.* 2008; 135:825–837. [PubMed: 19041748]
21. Haney EM, Warden SJ. Skeletal effects of serotonin (5-hydroxytryptamine) transporter inhibition: evidence from clinical studies. *J Musculoskelet Neuronal Interact.* 2008; 8:133–145. [PubMed: 18622082]
22. ten Berge D, Brugmann SA, Helms JA, et al. Wnt and FGF signals interact to coordinate growth with cell fate specification during limb development. *Development.* 2008; 135:3247–3257. [PubMed: 18776145]
23. Gabet Y, Noh T, Cogan J, et al. Crosstalk between androgen receptor and Wnt signaling mediates sexual dimorphism during bone mass accrual. *J Bone Miner Res.* 2008; 23:S35.
24. Hou X, Tan Y, Li M, et al. Canonical Wnt signaling is critical to estrogen-mediated uterine growth. *Mol Endocrinol.* 2004; 18:3035–3049. [PubMed: 15358837]
25. Pepersack T, Corvilain J, Bergmann P. Effects of lithium on bone resorption in cultured foetal rat long-bones. *Eur J Clin Invest.* 1994; 24:400–405. [PubMed: 7957493]
26. Yaccoby S, Ling W, Zhan F, et al. Antibody-based inhibition of DKK1 suppresses tumor-induced bone resorption and multiple myeloma growth in vivo. *Blood.* 2007; 109:2106–2111. [PubMed: 17068150]



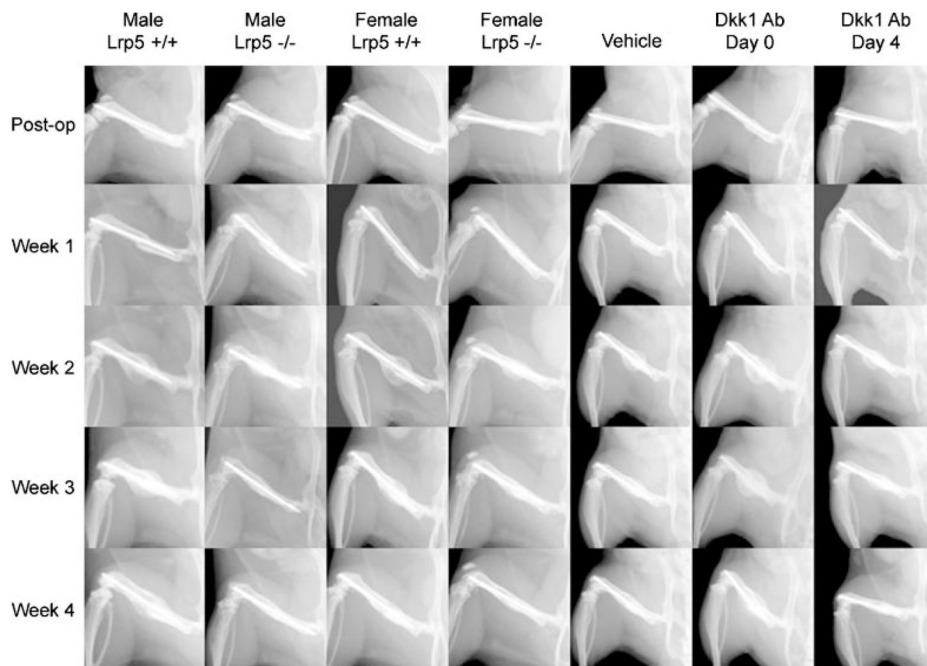


**Figure 1.** Longitudinal radiographs. Representative longitudinal radiographs from male and female Lrp5<sup>-/-</sup> and Lrp5<sup>+/+</sup> mice, as well as male mice treated with vehicle, Dkk1 Ab Day 0, and Dkk1 Ab Day 4. Radiographs are arranged by group (columns) and by time-point (rows). Each longitudinal series depicts the same animal at each of the indicated time points.

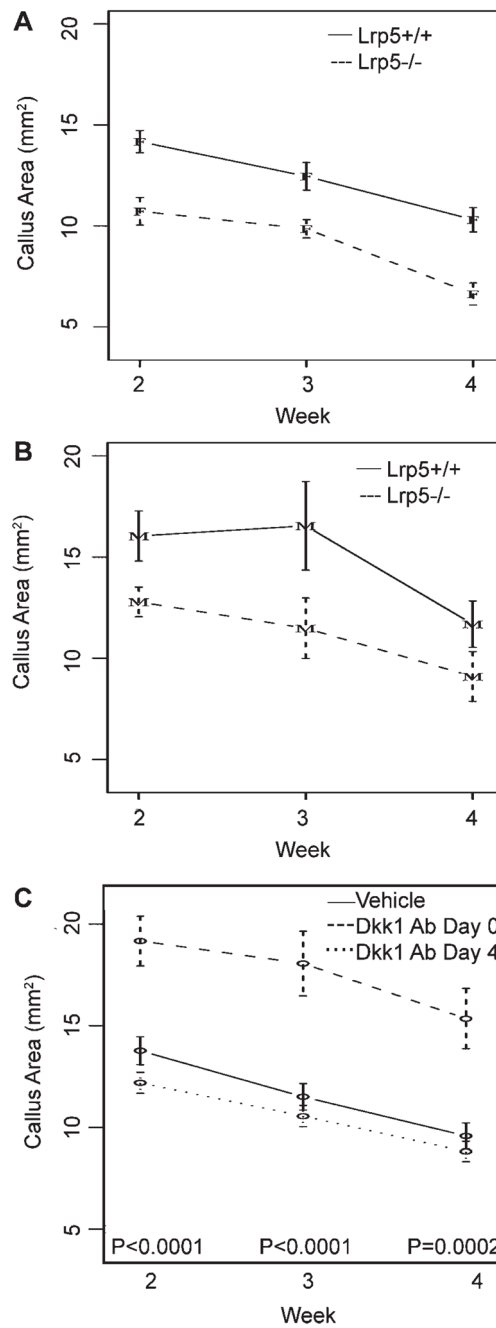


**Figure 2.** Longitudinal analysis of callus area. Graphs depicting mean callus area, measured from digital radiographs, over weeks 2, 3, and 4 for: (A) Female Lrp5+/+ and Lrp5-/- mice; (B) male Lrp5+/+ and Lrp5-/- mice and; (C) vehicle and Dkk1 Ab-treated mice. Error bars are  $\pm 1$  SEM.  $p$ -Values for tests of differences between genotypes (Lrp5+/+ vs. Lrp5-/-) are  $p = 0.0009$  at week 2,  $p = 0.0039$  at week 3, and  $p = 0.0048$  at week 4.  $p$ -Values for tests of differences among treatments (vehicle vs. Dkk1 Ab Day 0 vs. Dkk1 Ab Day 4) are indicated on the graph.

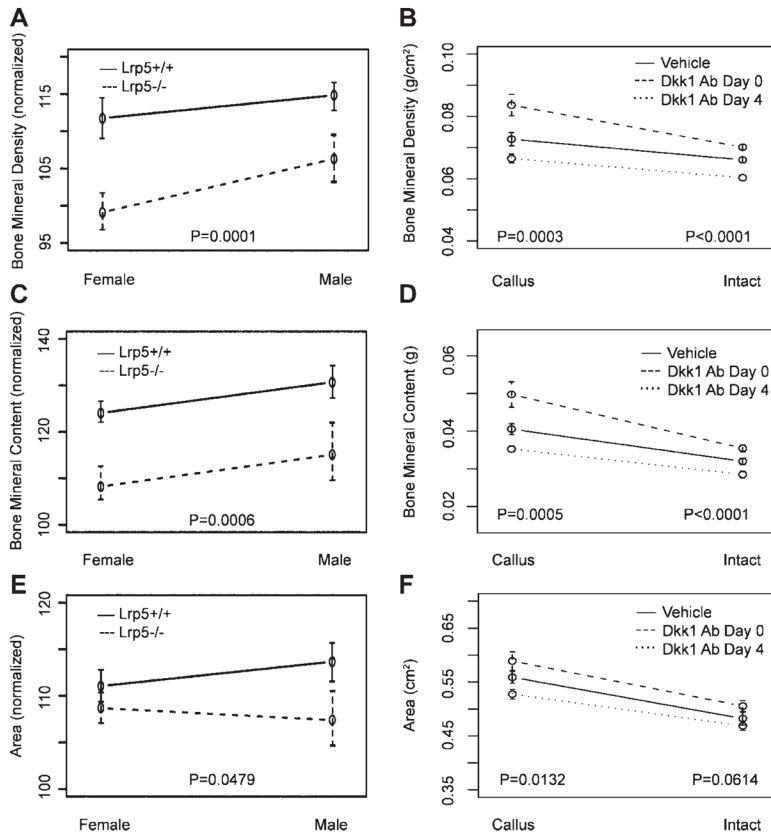


**Figure 3.** Dual-energy X-ray absorptiometry (DXA). Graphs illustrating average femoral BMD, BMC, and area of isolated femora as determined by DXA analyses. All raw values were normalized to contralateral intact values for analysis of genotype and sex effects (A–C). Actual values are reported for both intact and fractured (callus) femurs from vehicle and Dkk1 Ab-treated mice (D–F). Error bars are  $\pm 1$  SEM. *p*-Values for tests of differences between genotypes (Lrp5+/+ vs. Lrp5-/-) and among treatments (vehicle vs. Dkk1 Ab Day 0 vs. Dkk1 Ab Day 4) are given.

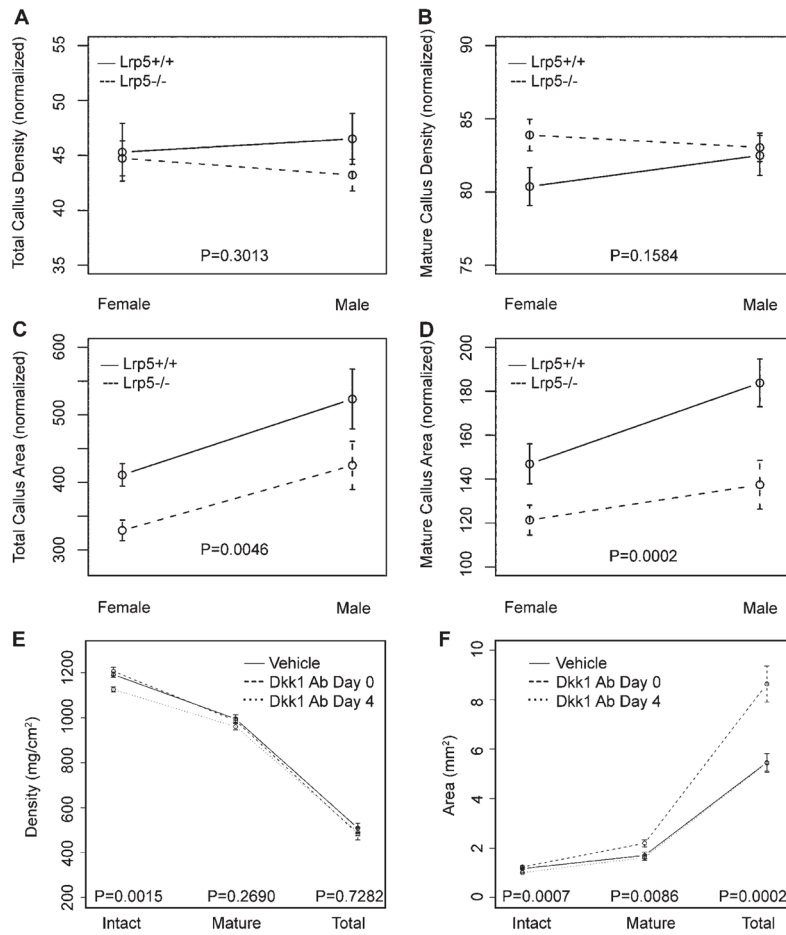


**Figure 4.** Peripheral quantitative computed tomography (pQCT). Series of graphs showing average cross-sectional density and area obtained from pQCT scanning of intact and fractured femora. All raw values were normalized to contralateral intact values for analysis of genotype and sex effects (A–C). Actual values are reported for both intact and fractured (callus) femurs from vehicle and Dkk1 Ab-treated mice (E, F). Error bars are  $\pm 1$  SEM. *p*-Values for tests of differences between genotypes (Lrp5+/+ vs. Lrp5-/-) and among treatments (vehicle vs. Dkk1 Ab Day 0 vs. Dkk1 Ab Day 4) are given.

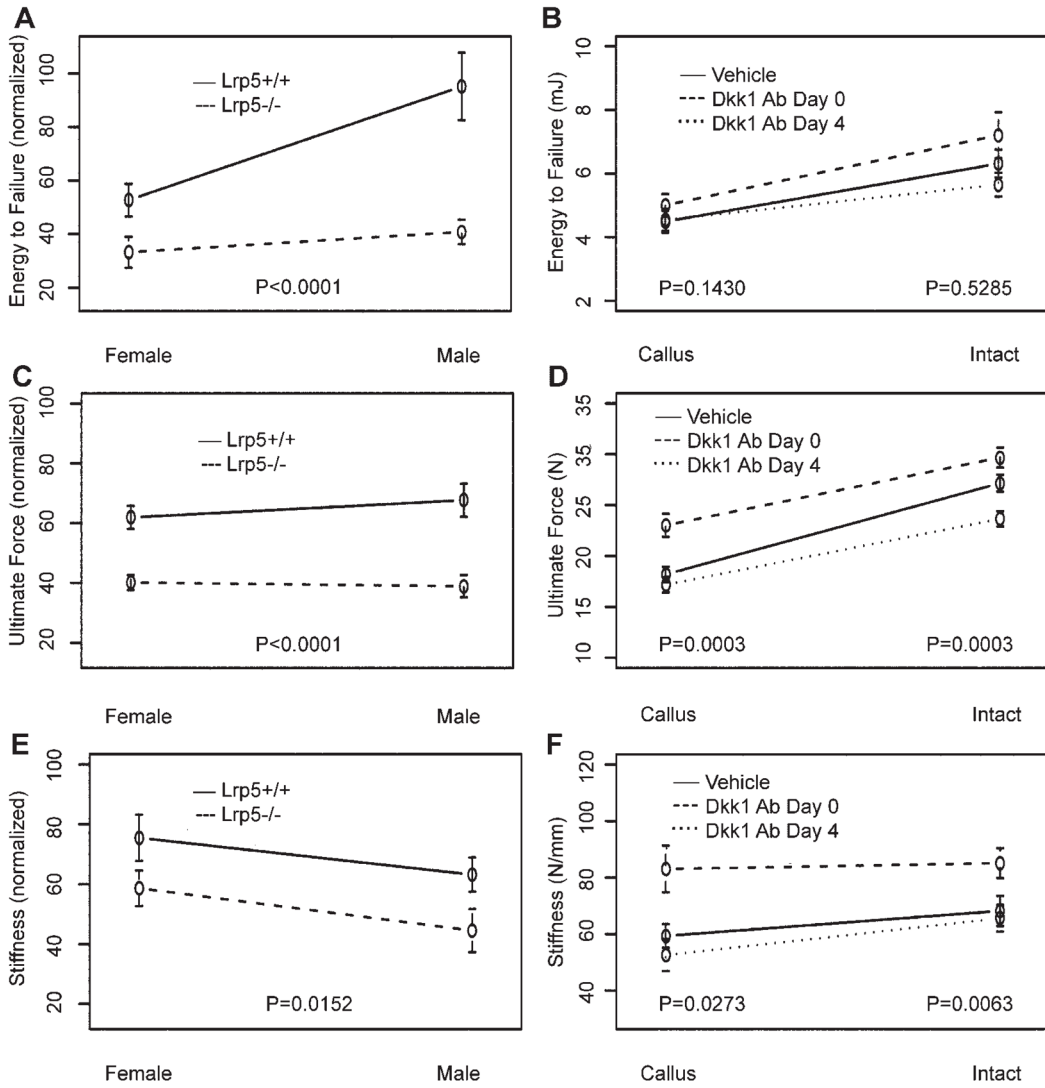


**Figure 5.** Biomechanical properties. Results of 4-point bending tests used to determine biomechanical properties of energy to failure, strength and stiffness of intact and fractured femora. All raw values were normalized to contralateral intact values for analysis of genotype and sex effects (A–C). Actual values are reported for both intact and fractured (callus) femurs from vehicle and Dkk1 Ab-treated mice (D–F). Error bars are  $\pm 1$  SEM. *p*-Values for tests of differences between genotypes (Lrp5<sup>+/+</sup> vs. Lrp5<sup>-/-</sup>) and among treatments (vehicle vs. Dkk1 Ab Day 0 vs. Dkk1 Ab Day 4) are given.

Table 1

DXA, pQCT, and Biomechanical Testing Results<sup>a</sup>

	Male Lrp5 +/+	Male Lrp5 -/-	Female Lrp5 +/+	Female Lrp5 -/-
DXA				
Callus BMD (g/cm <sup>2</sup> )	0.0792 ± 0.0101	0.0551 ± 0.0110	0.0787 ± 0.0083	0.0594 ± 0.0063
Callus BMC (g)	0.043 ± 0.008	0.026 ± 0.009	0.040 ± 0.005	0.029 ± 0.006
Callus area (cm <sup>2</sup> )	0.54 ± 0.04	0.46 ± 0.07	0.50 ± 0.02	0.47 ± 0.04
Intact BMD (g/cm <sup>2</sup> )	0.0691 ± 0.0088	0.0515 ± 0.0061	0.0704 ± 0.0037	0.0599 ± 0.0031
Intact BMC (g)	0.033 ± 0.007	0.022 ± 0.004	0.032 ± 0.004	0.026 ± 0.002
Intact area (cm <sup>2</sup> )	0.48 ± 0.04	0.43 ± 0.03	0.45 ± 0.03	0.44 ± 0.03
Total callus area (mm <sup>2</sup> )	6.40 ± 2.48	3.72 ± 1.21	4.76 ± 0.79	3.14 ± 0.64
Total callus BMD (mg/cm <sup>3</sup> )	587.2 ± 116.7	507.0 ± 79.4	575.4 ± 104.2	537.7 ± 72.6
Mature callus area (mm <sup>2</sup> )	2.23 ± 0.64	1.24 ± 0.47	1.72 ± 0.45	1.16 ± 0.29
Mature callus BMD (mg/cm <sup>3</sup> )	1039.7 ± 58.8	970.4 ± 71.7	1019.1 ± 40.7	1006.9 ± 39.9
Intact area (mm <sup>2</sup> )	1.21 ± 0.18	0.89 ± 0.15	1.16 ± 0.13	0.95 ± 0.09
Intact BMD (mg/cm <sup>3</sup> )	1262.1 ± 51.7	1168.7 ± 70.9	1268.4 ± 31.6	1201.5 ± 36.5
Biomechanics				
Callus energy to failure (mJ)	5.41 ± 2.95	1.54 ± 0.73	3.00 ± 1.02	1.44 ± 0.67
Callus stiffness (N/mm)	59.10 ± 31.22	28.01 ± 13.19	75.69 ± 25.93	39.59 ± 11.68
Callus ultimate load (N)	20.46 ± 8.94	7.66 ± 2.89	18.00 ± 4.32	8.98 ± 2.27
Intact energy to failure (mJ)	5.90 ± 1.90	3.85 ± 1.17	5.82 ± 1.15	4.55 ± 1.07
Intact stiffness (N/mm)	93.98 ± 36.93	66.91 ± 14.95	99.50 ± 13.83	68.38 ± 6.46
Intact ultimate load (N)	29.82 ± 7.23	19.61 ± 4.22	28.93 ± 3.10	22.20 ± 2.29

DXA, dual-energy X-ray absorptiometry; pQCT, peripheral quantitative computed tomography; Lrp, low-density lipoprotein receptor-related protein; BMD, bone mineral density; BMC, bone mineral content.

<sup>a</sup>This table lists the actual values for each of the parameters calculated following DXA, pQCT, and biomechanical analyses of fractured and intact femora from male and female Lrp5<sup>+/+</sup> and Lrp5<sup>-/-</sup> mice. All data are presented as group average ± SD.